Network Model of the CPE

Juraj VALSA[1], *Petr DVOŘÁK*[2], *Martin FRIEDL*[1]

[1]Dept. of Theoretical and Experimental El. Engineering, Brno Univ. of Technology, Kolejní 8, 612 00 Brno, Czech Rep.
[2]Dept. of Electrical and Electronic Technology, Brno University of Technology, Technická 10, 612 00 Brno, Czech Rep.

valsa@feec.vutbr.cz, dvorakp@feec.vutbr.cz, friedl@feec.vutbr.cz

Abstract. *Analysis of fractal systems (i.e. systems described by fractional differential equations) necessitates to create an electrical analog model of a crucial subsystem called Constant Phase Element (CPE). The paper describes a possible realization of such a model that is quite simple and in spite of its simplicity makes it possible to simulate the properties of ideal CPEs. The paper also deals with the effect of component tolerances on the resultant responses of the model and describes several typical model applications.*

Keywords

Fractional differential equations, Constant Phase Element, Warburg impedance.

1. Introduction

A classical description of dynamics of processes in physical systems is based on differential equations with state variables and their derivatives and integrals. The solution procedures of these equations have been developed for past decades and centuries and are considered standard at present.

During the investigations in many scientific disciplines, it proved that the mentioned classical methods do not suffice. There exist phenomena that are not accurately depicted and therefore it is necessary to apply differential equations with derivatives and integrals of noninteger orders [1-5]. These are fractional differential equations and the question is how to solve them.

The phenomena described by such equations are frequent for instance in biochemistry or biomedicine [6-8], in electrochemistry [9], [10], in modern control technique [11-15], in acoustic or optical signal processing [16], [17] and in many other practical domains.

If the fractional equations are sufficiently simple then it is possible to solve them with the help of special functions [2]. In case of linear systems the solution may be based very effectively on Laplace transformation, namely on numerical methods of inversion [2], [19], [23]. For solution of nonlinear systems there exist numerical methods of integration.

The solution of many practical problems can be simplified with the help of electrical or electronic analog models. Formulation of effective models of fractional systems is the substance of this paper.

The paper has the following structure: In section 2 the ideal Constant Phase Element (CPE) is defined. Section 3 presents the basic electrical scheme of the model and describes its general properties. In section 4, the principle of correction of characteristics of the model is explained and it is shown that it is possible to improve the model properties markedly with a minimum of additional components. The analysis of effect of component tolerances on the resultant model responses is contained in section 5. Several examples of practical applications of the described models are shown in section 6. List of most important references concludes the paper.

2. Ideal Constant Phase Element (CPE)

The impedance of an ideal CPE is defined as

$$Z(s) = Ds^{\alpha} . \tag{1}$$

For $s = j\omega$ will then be

$$\begin{aligned}\hat{Z}(j\omega) &= D(j\omega)^{\alpha} = D\omega^{\alpha} j^{a} = D\omega^{\alpha} e^{j\varphi} = \\ &= D\omega^{a}(\cos\varphi + j\sin\varphi)\end{aligned} \tag{2}$$

$\varphi = \alpha\dfrac{\pi}{2}$ for φ in radians or $\varphi = 90\alpha$ for φ in degrees.

The exponent α decides the character of the impedance $Z(s)$. If $\alpha = +1$, it is a classical inductive reactance, $\alpha = 0$ means a real resistance or conductance, $\alpha = -1$ represents a classical capacitive reactance.

The values $0 < \alpha < 1$ corresponds to a fractal inductor, the value $-1 < \alpha < 0$ to a fractal capacitor. This paper is devoted predominantly to the fractal capacitor.

The modulus of impedance $\hat{Z}(j\omega)$ depends on frequency according to the magnitude of α. Its value in decibels varies with 20α decibels per decade of frequency and in correspondence with the sign of α, the modulus increases or decreases.

At $\omega = 1$ the modulus equals D with no respect to α.

Argument φ of the impedance is constant, frequency independent.

It is evident that the properties of ideal CPE cannot be realized with classical electrical networks containing a finite number of discrete R, C, L components. On the other hand, it is possible to build networks that approximate the CPE in a reasonable way. During the second half of the 20th century many attempts to implement such an approximation were published, see for instance [5]. It turned out however that these attempts were not too successful. The design starts with s^α approximation by an infinite series or chain fraction and necessitates partial fraction decomposition together with calculation of denominator roots and even demands optimization steps. The resultant network is very complicated [20], may demand components with negative parameters or a number of active elements.

Therefore, there is a need to find a simple design of a reasonably accurate CPE model.

3. Basic Network Model

The following text is based on the paper [22]. Basic structure of the model is shown in Fig.1.

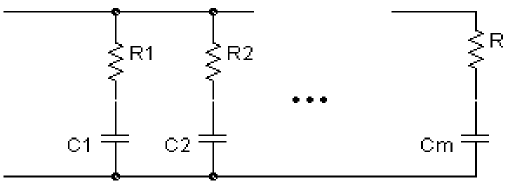

Fig. 1. Basic network model.

The network consists of altogether m series RC branches connected in parallel. The resistances and capacitances in branches form a geometric sequence

$$R_k = R_1 a^{k-1},\ C_k = C_1 b^{k-1},\ k = 1, 2, ..., m \tag{3}$$

and for the coefficients a and b it holds

$$0 < a < 1,\ \ 0 < b < 1.$$

Input impedance of the network $Z(j\omega) = 1/Y(j\omega)$, where $Y(j\omega)$ is input admittance equal to the sum of admittances of individual branches

$$Y(j\omega) = \sum_{k=1}^{m} \frac{j\omega b^{k-1} C_1}{1 + j\omega (ab)^{k-1} R_1 C_1}\,. \tag{4}$$

The modulus of input impedance in decibels equals

$$Z_{dB}(\omega) = 20 \log |Z(j\omega)| \tag{5}$$

and argument in degrees

$$\varphi(\omega) = \frac{180}{\pi} arctg \frac{imag(Z(j\omega))}{real(Z(j\omega))}\,. \tag{6}$$

A typical example of both characteristics for the case $R_1 = 1$, $C_1 = 1$, $m = 10$, $a = 0.25$, $b = 0.48$ is shown in Fig. 2.

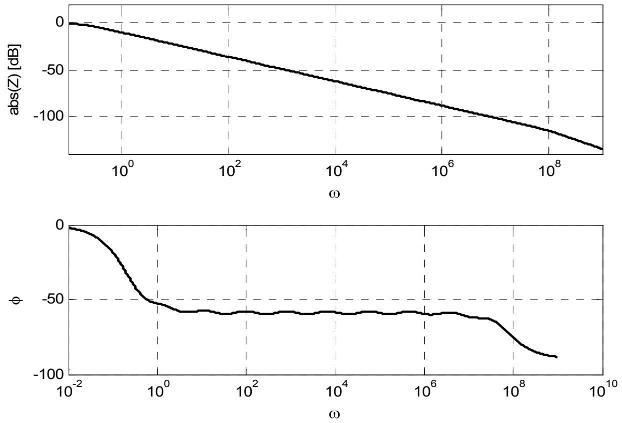

Fig. 2. Modulus and argument as function of frequency.

The figures show that under the presented conditions the network is able to simulate the ideal CPE at least in a limited band of frequencies approximately from $\omega_d = 10^1$ to $\omega_h = 10^7$. The modulus decreases with the rate -13 dB per decade and for $\omega = 1$ it equals -10 dB ($D = 10^{-0.5} = 0.316$). The argument has average value $\varphi_{av} = -59°$ and oscillates around it with amplitude $\Delta\varphi = \pm 1°$.

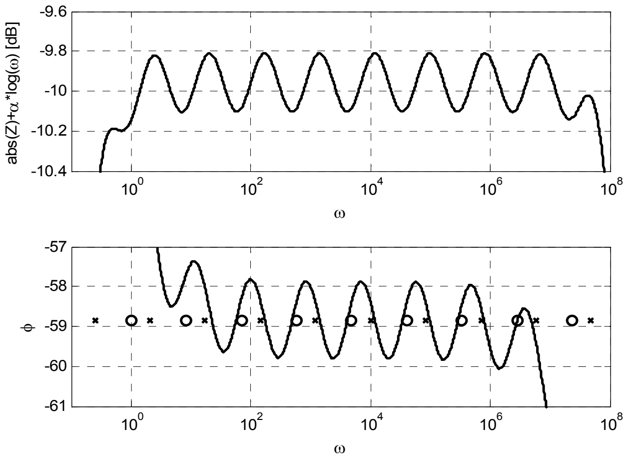

Fig. 3. Details of modulus and phase.

The modulus response in the original scale does not clearly show the ripple around the average curve. After adding the component with corresponding slope we get clearer idea about the real situation. The detailed shapes of both the responses are shown in Fig. 3.

The a and b parameters, as will be shown later, determine φ_{av}, $\Delta\varphi$, ω_d, ω_h and D.

Under the supposition of a sufficient number m of sections it is possible to derive easily the basic relations for the network properties in the frequency range of interest. The reasoning starts with the asymptotic Bode characteristics.

The modulus characteristic of the k-th section consists of a part with the slope of 20dB/decade and of another part with zero slope. The breaking point lies at frequency equal to $\omega_k = z_k = 1/\tau_k = 1/R_k C_k$. The breaking point of the following section lies at $\omega_{k+1} = \omega_k /(ab)$. At the logarithmic scale the breaking frequencies are equidistant. The just described situation is periodically repeated.

The resultant admittance equals the sum of individual admittances

$$Y(s) = \sum_{k=1}^{m} \frac{s b^{k-1} C_1}{1 + s(ab)^{k-1} R_1 C_1}. \tag{7}$$

The input impedance $Z(s) = 1/Y(s)$ has zeros at the breaking points

$$z_k = \frac{1}{R_1 C_1 (ab)^{k-1}}, \; k = 1,...,m \tag{8}$$

and poles

$$p_k = \frac{z_k}{b}, \; z_{k+1} = \frac{p_k}{a}. \tag{9}$$

An example of zeroes and poles distribution is shown in Fig. 3 (zeroes are denoted with circles, poles with crosses).

For $s = j\omega$ is then

$$Y(j\omega) = \sum_{k=1}^{m} \frac{j\omega b^{k-1} C_1}{1 + j\omega(ab)^{k-1} R_1 C_1}, \quad Z(j\omega) = 1/Y(j\omega). \tag{10}$$

Argument $\varphi(\omega)$ of $Z(j\omega)$ in degrees is

$$\varphi(\omega) = \frac{180}{\pi} arctg(imag(Z)/real(Z)) \; . \tag{11}$$

Its average value can be obtained as (see [22])

$$\varphi_{av} = 90\alpha = 90 \frac{\log a}{\log a + \log b} = 90 \frac{\log a}{\log(ab)} \; . \tag{12}$$

The phase characteristic passes values φ_{av} in the points of

$$\omega_{av}(k) = z_k \left(\frac{a}{b}\right)^{1/4} \tag{13}$$

and reaches its extremes at

$$\omega_{\varphi\min}(k) = z_k \sqrt{a} \quad \text{or} \quad \omega_{\varphi\max}(k) = p_k \sqrt{b} = \frac{z_k}{\sqrt{b}}. \tag{14}$$

Evidently it holds $\omega_{av} = \sqrt{\omega_{\varphi\min}\omega_{\varphi\max}}$, (15)

the frequencies ω_{av} are in the middle (on logarithmic scale) between the frequencies of extremes.

The values $\omega_{\varphi\min}$ and $\omega_{\varphi\max}$ are simultaneously frequencies where the modulus has its average value equal to that of the ideal CPE.

4. The Principle of the Optimal Model

The preceding section 3 presented a model with characteristics simulating well those of an ideal CPE. The model however necessitates a relatively high number of sections to secure a good approximation in the given frequency range. Fig. 4 demonstrates that if $m < 10$ the results are not satisfactory at all.

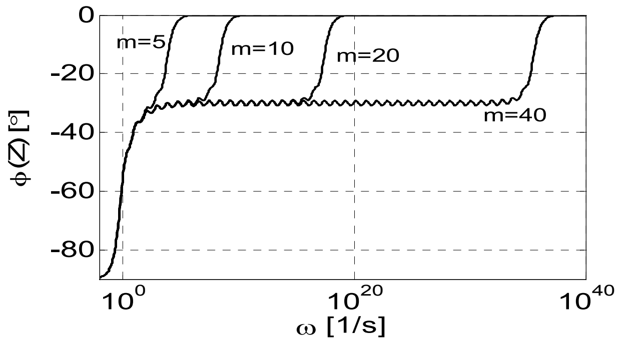

Fig. 4. Phase responses with different number of sections.

We shall show a possibility how to reduce the complexity of the model and preserve at the same time its required good qualities.

Fig. 5a shows that at a certain frequency different sections contribute to the total input current (and to resultant input admittance) with different weight. The resultant input current is determined by a limited number of sections. Fig. 5b and 5c make it clear that at both ends of the frequency range the normal operating conditions are not satisfied since the necessary sections are missing. At the lower end they are the sections with indexes $k < 1$, at the upper end the sections $k > m$. For the model to operate correctly it is necessary to substitute the missing sections (we suppose an infinite number of them at both ends of the frequency range) by a simple network. The missing sections at the lower end have large time constants. Their capacitances can thus be neglected and the conductances

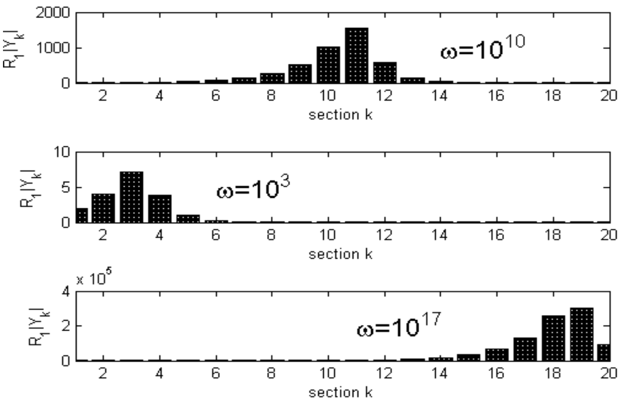

Fig. 5. Relative contribution of individual sections to the total current: a. Middle frequency, b. Low frequency, c. High frequency

added. As the values of conductances form a geometric sequence the infinite sum of them can be substituted with a single

$$G_p = \frac{1}{R_1} \sum_{k=1}^{\infty} a^k = \frac{1}{R_1} \frac{a}{1-a} \tag{16}$$

or a single resistor

$$R_p = R_1 \frac{1-a}{a}. \tag{17}$$

Similarly, at the upper end a single capacitor will suffice

$$C_p = C_1 \frac{b^m}{1-b}. \tag{18}$$

The resultant electrical scheme of the model is in Fig. 6.

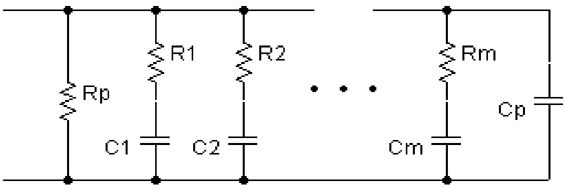

Fig. 6. Resultant scheme with correcting elements R_p and C_p.

The substitute is not perfect since the original parallel combinations of series *RC* sections were replaced by two single components. The resultant characteristics are however much better than those of the original model without the corrective elements.

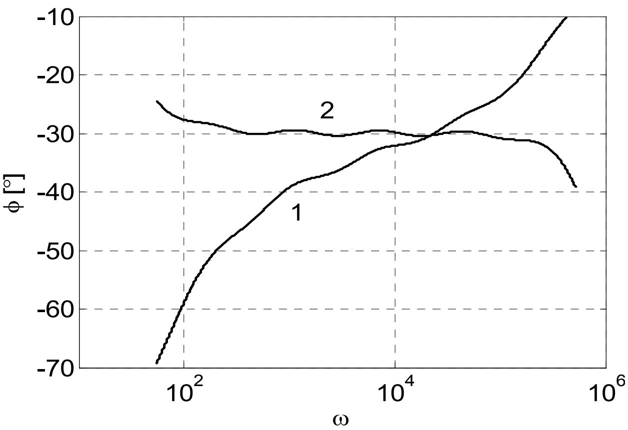

Fig. 7. Comparison of phase responses; uncorrected model (curve 1), model with correction elements (curve 2).

Fig. 7 compares the phase responses of the model with $m = 5$, $\varphi = -30°$ without and with correction. Obviously, the original model is not applicable while that with correcting elements is quite good. The phase is virtually constant over the frequency range covering nearly 3 decades. The model contains only 6 resistors and 6 capacitors. The frequency band may be easily extended by adding further sections and recalculating the capacitance C_p.

	ideal	uncorrected	corrected
1	-0.54288	0	-0.49213
2	-3.3931	-2.5885	-3.3760
3	-21.207	-18.806	-21.198
4	-132.55	-127.18	-132.57
5	-828.42	-866.16	-832.57
6	-5177.7		-8814.8

Tab. 1. Position of impedance poles without and with correcting elements.

The effect of correcting elements can be understood even from Tab. 1, showing the positions of poles of input impedance (the positions of zeroes are not affected). The table confirms that the correction substantially contributes to the ideal pole positions defined by (9).

4.1 Design Procedure

The graph in Fig. 8, obtained as a result of computer simulations, shows how phase φ and ripple $\Delta\varphi$ depend on basic *a* and *b* parameters. It is evident that at least between $\varphi = -30°$ and $\varphi = -60°$ the ripple is connected with the product *ab*. In the figure, three important cases are depicted: for $\Delta\varphi = \pm 0.5°$ the product $ab = 0.160$ (asterisks in Fig. 8), for $\Delta\varphi = \pm 1°$, $ab = 0.12$ (crosses) and for $\Delta\varphi = \pm 2°$ $ab = 0.08$ (dots).

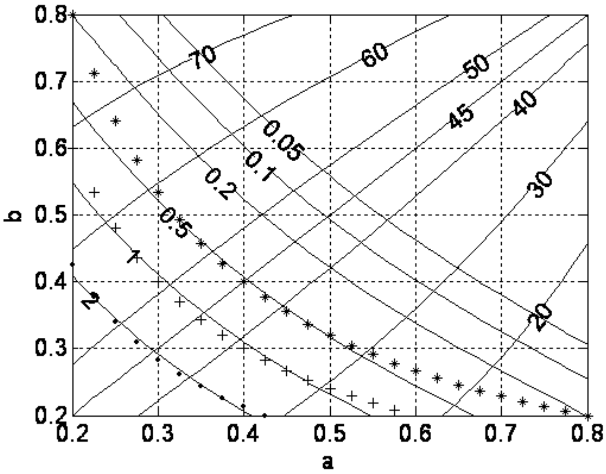

Fig. 8. Dependence of phase φ and ripple $\Delta\varphi$ on parameters *a* and *b*.

The design of the model starts with the given $\tau_1 = R_1C_1$, φ_{av}, $\Delta\varphi$, m, D_p .

Time constant τ_1 together with the number *m* approximately determines both end frequencies

$$\omega_d = \frac{1}{\tau_1}, \quad \omega_h = \frac{1}{\tau_1 (ab)^m} = \frac{\omega_d}{(ab)^m}. \tag{19}$$

Allowable ripple $\Delta\varphi$ leads to

$$ab \cong \frac{0.24}{1+\Delta\varphi} \tag{20}$$

where $\Delta\varphi$ is in degrees. Starting with

$$\alpha = \varphi / 90,$$
$$\log a = \alpha \log(ab), \quad a = 10^{\log a}, \quad b = ab / a.$$

we determine the values of resistors and capacitors in sections

$$R_k = R_1 a^{k-1}, \quad k = 1, 2, \ldots m$$
$$C_k = C_1 b^{k-1}, \quad k = 1, 2, \ldots m$$

and the correction elements

$$R_p = R_1 \frac{1-a}{a}, \quad C_p = C_1 \frac{b^m}{1-b}.$$

For the chosen values of R_1 and C_1 we get the input admittance

$$Y(j\omega_{av}) = \frac{1}{R_p} + j\omega_{av} C_p + \sum_{k=1}^{m} \frac{j\omega_{av} C_k}{1 + j\omega_{av} R_k C_k}$$

at the some of the frequencies of phase extremes, for instance, according to (13)

$$\omega_{av} = z_k \sqrt{a} = \frac{1}{R_1 C_1 (ab)^{k-1}} \sqrt{a}, \qquad k = \text{int}(m/2) \tag{21}$$

Since the slope of the modulus is proportional to α we get the modulus D at $\omega = 1$ as

$$D = Z_{av} \omega_{av}{}^{-\alpha} \tag{22}$$

where

$$Z_{av} = \frac{1}{|Y(j\omega_{av})|} \tag{23}$$

is modulus at $\omega = \omega_{av}$.

The obtained value of D will generally differ from the required D_p. Therefore, all values of resistances in sections R_k and R_p have to be multiplied by ratio D_p/D and all capacitances divided by the same ratio. Time constant $\tau_1 = R_1 C_1$ and limits of the frequency range remain unchanged.

4.2 Example

Given

R_1= 10 kΩ, C_1= 1 μF, (τ_1= 10 ms), φ = -30°,

D_p=10^4, m = 5, $\Delta\varphi$ = 0.5.

Set

$ab = 0.24/(1 + \Delta\varphi) = 0.160$,

$a = 10^{\alpha \log(ab)} = 0.54288, \quad b = ab/a = 0.29472$,

$$R_p = \frac{R_1(1-a)}{a} = 8420.1\,\Omega,$$

$$C_p = \frac{C_1 b^m}{1-b} = 3.1529 \text{ nF},$$

$$\omega_{av} = \left(\frac{a}{b}\right)^{0.25} \frac{1}{R_1 C_1 (ab)^2} = 4550.8, \quad Z_{av} = 1401.1\,\Omega,$$

$$D = 1404.1 \times 4550.8^{-(30/90)} = 23268,$$

$$D_p / D = 10^4 / 23268 = 0.42978,$$

thus R_1= 4297.8 Ω, C_1= 10^{-6}/0.42978 = 2.33 μF,
R_2 = 2333.2 Ω, R_3 = 1266.7 Ω, R_4 = 687.7 Ω, R_5 = 373.3 Ω,
C_2 = 686 nF, C_3 = 202 nF, C_4 = 59.6 nF, C_5 = 17.6 nF,
R_p= 3619 Ω, C_p= 7.34 nF.

The phase response of the model is flat approximately from ω_d= 300, (f_d= 50 Hz) to ω_h= 10^5 (f_d= 16 kHz).

The just described design procedure is straightforward and very simple. It does not require any complicated optimization steps or operations with chain- or partial fractions. It results in ordinary off-the-shelf resistors and capacitors without operational amplifiers.

4.3 Alternative Series Model

For some applications, another model in Fig. 9 may be more advantageous.

Its input impedance

$$Z(j\omega) = R_s + \sum_{k=1}^{m} \frac{R_k}{1 + j\omega R_k C_k} + \frac{1}{j\omega C_s}, \tag{24}$$

with resistances and capacitances in individual parallel RC circuits

$$R_k = R_1 a^{k-1}, \ C_k = C_1 b^{k-1}, \tag{25}$$

and correcting elements

$$R_s = R_1 \frac{a^m}{1-a}, \ C_s = C_1 \frac{1-b}{b}. \tag{26}$$

The argument response of this model reasonably corresponds to that of the previous variant.

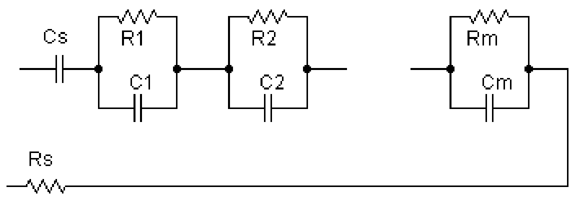

Fig. 9. Scheme of a series model.

5. Effect of Component Tolerances on the Model Responses

When realizing the network model in practice one necessarily meets the problem with component tolerances. The calculated component values will unavoidably differ from the stock values delivered in standard series and the influence of environmental and temperature changes has also to be taken into consideration.

For objective evaluation of such effects, the calculation of sensitivities serves best.

Absolute sensitivity of the input impedance Z_{in}= U_{in}/I_{in} to the variation of admittance Y_q is defined as

$$S(Z_{in}, Y_q) = \frac{\partial Z_{in}}{\partial Y_q}. \tag{27}$$

The so-called semirelative sensitivity (change of Z_{in} caused by a relative change of Y_q) is

$$\mathrm{S_r}(Z_{in},Y_q)=\frac{\partial Z_{in}}{\dfrac{\partial Y_q}{Y_q}}=Y_q S(Z_{in},Y_q) \qquad (28)$$

The partial derivative in (27) can be obtained as negatively taken product of transfer impedance from input to the terminals of Y_q and transfer impedance taken in reverse direction [23]. Due to the reciprocity of the CPU model, the two named transfer impedances equal each other and their product equals the transfer impedance Z_t from input to Y_q squared.

$$S_{Y_q}(Z_{in},Y_q)=\frac{\partial Z_{in}}{\dfrac{\partial Y_q}{Y_q}}= \\ =Y_q S(Z_{in},Y_q)=-Y_q(Z_t)^2 \qquad (29)$$

and the sensitivity of phase to Y_q will be [23]

$$S_{Y_q}(\varphi,Y_q)=\frac{\partial\varphi}{\dfrac{\partial Y_q}{Y_q}}=imag\left(\frac{S_{Y_q}(Z_{in},Y_q)}{Z_{in}}\right). \qquad (30)$$

Fig. 10 shows an example of semirelative sensitivities of phase to component values for the case $m = 5$, R_1= 10 kΩ, C_1= 1 μF. Evidently, a 10% tolerance of any component will not cause (in the frequency band of interest) greater phase error than about 1 degree.

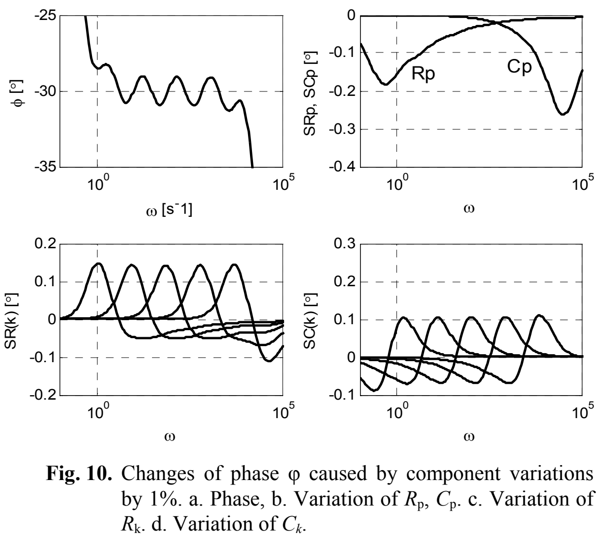

Fig. 10. Changes of phase φ caused by component variations by 1%. a. Phase, b. Variation of R_p, C_p. c. Variation of R_k. d. Variation of C_k.

6. Some Applications of the CPE Models

A good CPE model can be used for simulation and experimental verification of properties of various fractal systems. In connection with operational amplifiers, it makes it possible to build analog networks described by fractional differential equations. The simplest networks of this kind are fractional differentiator and fractional integrator. Their schemes are in Fig. 11.

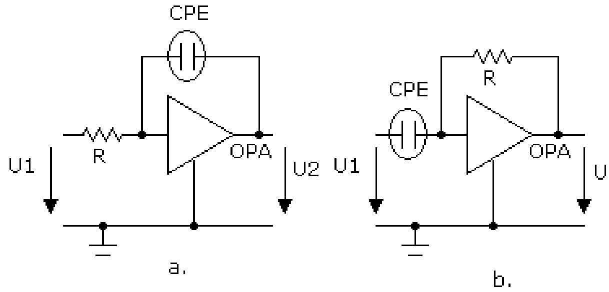

Fig. 11. Fractional analog integrator and differentiator.

Voltage transfer factor of the fractional integrator is

$$K(s)=-\frac{D}{s^{|\alpha|}R},\quad -1<\alpha<0 \qquad (31)$$

while that of the differentiator

$$K(s)=-s^{|\alpha|}\frac{R}{D},\quad -1<\alpha<0. \qquad (32)$$

With the help of these simple circuits it is possible to perform analog operations with electric signals.

Fig. 12 compares as an example the "ideal" fractional derivatives of signal $A\sin t$, $0 < t < \pi$, for α = -0,3, α = -0,5, α = -0,7, α = -1 (classical 1[st] derivative $A\cos t$) with the output of the analog differentiator (m = 4, time constant R_1C_1= 10 s, denoted with crosses). All the waveforms were obtained by numerical inversion of the corresponding Laplace transforms [19] under zero initial conditions. Obviously, the used relatively simple CPE model delivers very good results.

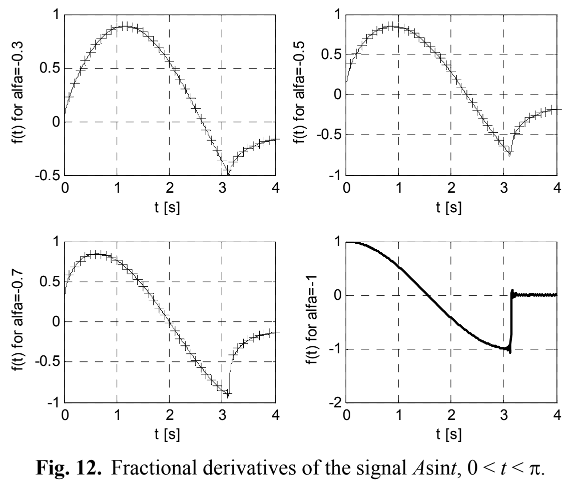

Fig. 12. Fractional derivatives of the signal $A\sin t$, $0 < t < \pi$.

Fig. 13 shows an analog model of a fractional regulation system [20] with transfer factor

$$K_u(s)=\frac{1}{1+0.5s^{0.9}+0.8s^{2.2}}= \\ =\frac{-1}{\dfrac{R_1}{R_{f2}}+\dfrac{R_1R_3}{R_{f1}D_3}s^{-\alpha_3}+\dfrac{R_1R_2R_3}{D_1D_2D_3}s^{-(\alpha_1+\alpha_2+\alpha_3)}} \qquad (33)$$

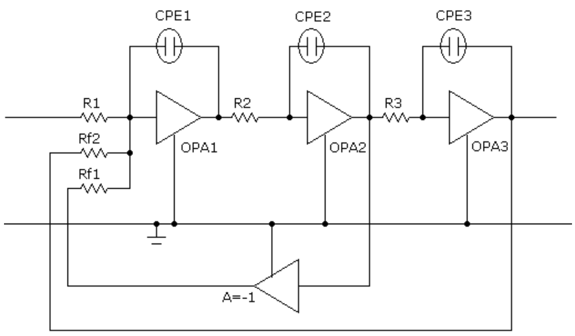

Fig. 13. Analog model of a fractional control system (33).

Parameters of individual CPEs used in the scheme are for instance α_1= -1 (the first stage is a classical integrator with the capacitor C= 1/D_1), α_2= -0.3, φ_2= -27°, α_3= -0.9, φ_3= -81°, R_1= R_{f2}.

Optimal PD controller should have transfer factor

$$K_c(s) = 20.5 + 3.7343 s^{1.15} . \qquad (34)$$

Its possible model is in Fig. 14.

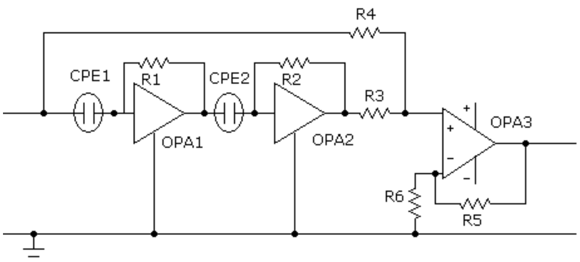

Fig. 14. Analog model of the controller (34).

Transfer factor of the controller in Fig. 14

$$K_c(s) = \frac{R_3 + R_4 \dfrac{R_1 R_2}{D_1 D_2} s^{|\alpha_1+\alpha_2|}}{R_3 + R_4}(1 + \frac{R_5}{R_6}),$$

$$-1 < \alpha_1 < 0, \ \ -1 < \alpha_2 < 0 . \qquad (35)$$

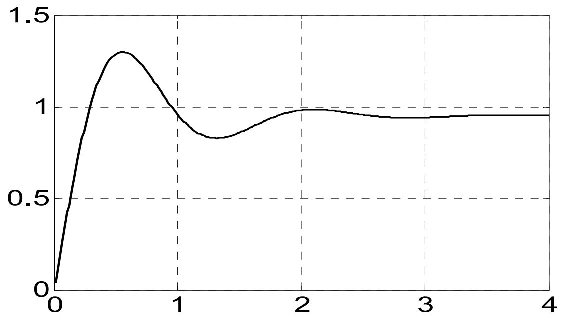

Fig. 15. Step response of the fractional control system with controller.

With α_1= -0.5, α_2= -0.65, the transfer factor of the complete system with controller will be

$$K(s) = \frac{K_s(s) K_c(s)}{1 + K_s(s) K_c(s)} = \\ = \frac{20.5 + 3.7343 s^{1.15}}{0.8 s^{2.2} + 3.7343 s^{1.15} + 0.5 s^{0.9} + 21.5} \qquad (36)$$

and its step response obtained by numerical inversion of 1/s K(s) and verified with the realized model is shown in Fig. 15.

Paper [7] presents an electrical model of intestine containing 2 ideal CPEs with different parameters. Its impedance obtained by approximation of measured data is

$$Z(s) = R_1 + \frac{R_2}{1 + \dfrac{R_2}{D_1 s^{\alpha_1}}} + \frac{R_3}{1 + \dfrac{R_3}{D_2 s^{\alpha_2}}} \qquad (37)$$

where R_1= 42.9 Ω, R_2= 71.6 Ω, R_3= 16.5 Ω, D_1= 324×10^3, α_1= -0.507, D_2= 11.2×10^3, α_2= -0.766.

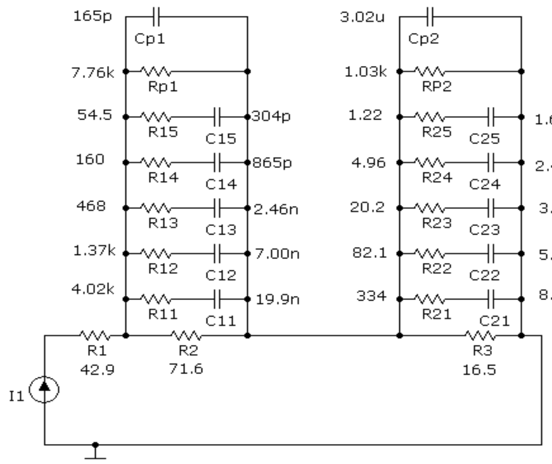

Fig. 16. Network model of impedance (37).

One possible realization of corresponding network model is shown in Fig. 16. Fig. 17 then presents the frequency response according to (37) together with the values of the network model.

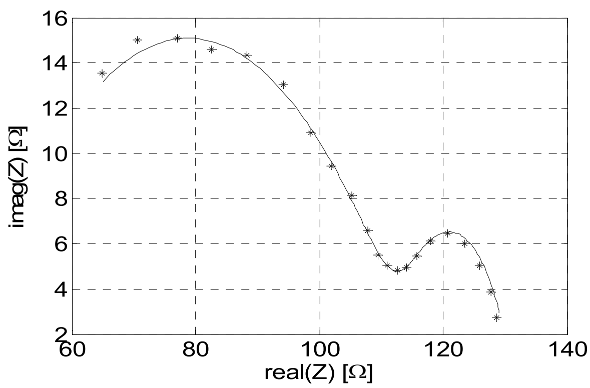

Fig. 17. Frequency responses of the intestine model; full line - equation (37), asterisks - network model in Fig. 16.

7. Conclusion

The paper presents a relatively simple yet still acceptably faithful network model of the CPE, built of off-the-shelf passive resistors and capacitors. Contrary to other known models its design does not need complicated optimization steps. Sensitivity analysis shows that standard component tolerances do not affect the properties of the model too much and the components need no special selection.

Acknowledgements

The research described in the paper was supported by the Ministry of Education (projects MSM0021630516 and MSM 0021630513), BUT Grant Agency FEKT-S-11-5 and by the EU (project CZ.1.05/2.1.00/01.0014).

References

[1] SCHROEDER, M. *Fractals, Chaos, Power Laws, Minutes from an Infinite Paradise.* New York: W. H. Freeman and Company, 1991.

[2] PODLUBNY, I. *Fractional Differential Equations.* San Diego: Academic Press, 1st edition, 1999.

[3] HILFER, R. (editor) *Applications of Fractional Calculus in Physics*. World Scientific Publishing Co., 2000.

[4] ORTIGUERA, M. D. An introduction to the fractional continuous-time linear systems: The 21st century systems, *IEEE Circuit and Systems Magazine*, 3rd quarter 2008.

[5] ELWAKIL, A. S. Fractional-order circuits and systems: An emerging interdisciplinary research area. *IEEE Circuit and Systems Magazine,* 4th quarter 2010.

[6] TANG, C., YOU, F., CHENG, G., GAO, D., FU, F., DONG, X. Modeling the frequency dependence of the electrical properties of the live human skull. *Physiol. Meas.*, 2009, vol. 30, p. 1293–1301.

[7] RIGAUD, B. et al: In vitro tissue characterization and modelling using electrical impedance measurements in the 100 Hz-10 MHz frequency range. *Physiol. Meas.,* 1995, vol. 16, p. A15-A28.

[8] IONESCU, C., DE KEYSER, R. Parametric models for characterizing respiratory input impedance. *J. Med. Eng. Technol.*, 2008, vol. 32, p..315–324.

[9] IONESCU, C., DE KEYSER, R. Relations between fractional-order model parameters and lung pathology in chronic obstructive pulmonary disease. *IEEE Trans. Biomed. Eng.*, 2009, vol. 56, p. 978–987.

[10] KÖTZ, R., CARLEN, M. Principles and applications of electrochemical capacitors. *Electrochimica Acta*, 2002, vol. 53, p. 2483–2498.

[11] BISQUERT, J., COMPTE, A. Theory of the electrochemical impedance of anomalous diffusion. *Electroanal. Chem.*, 2001, vol. 499, no. 1, p. 112–120.

[12] SKAAR, S. B., MICHEL, A. N., MILLER, R. K. Stability of viscoelastic control systems. *IEEE Trans. Automat. Contr.*, 1998, vol. 33, p. 348–357.

[13] PODLUBNY, I. Fractional-order systems and PID-controllers. *IEEE Trans. Automat. Contr.*, 1999, vol. 44, p. 208–214.

[14] PETRAS, I. The fractional order controllers: Methods for their synthesis and application. *J. Elect. Eng.*, 1999, vol. 50, p. 284–288.

[15] MACHADO, J. Discrete-time fractional-order controllers. *Fractional Calculus Appl. Anal.*, 2001, vol. 4, p. 47–66.

[16] PODLUBNY, I., VINAGRE, B., O'LEARY, P., DORČÁK, L. Analogue realizations of fractional-order controllers. *Nonlinear Dyn.*, 2002, vol. 29, p. 281–296.

[17] ORTIGUEIRA, M. D. Introduction to fractional signal processing. Part 1: Continuous-time systems. *IEE Proc. on Vision, Image and Signal Processing*, Feb. 2000, vol. 147, no. 1, p. 62–70.

[18] ORTIGUEIRA, M. D. Introduction to fractional signal processing. Part 2: Discrete-time systems. *IEE Proc. on Vision, Image and Signal Processing*, Feb. 2000, vol. 147, no. 1, p. 71–78.

[19] VALSA, J., BRANČÍK, L. Approximate formulae for numerical inversion of Laplace transforms. *Int. Journal for Numerical Modelling: Electronic Networks, Devices and Fields,* June 1998, vol. 11, p. 153-166.

[20] DORČÁK, L., TERPÁK, J., PETRÁŠ, I., DORČÁKOVÁ, F. Electronic realization of the fractional-order systems. *Acta Montanistica Slovaca,*2007, vol. 12, no. 3, p. 231-237.

[21] KAWABA et al. A Realization of fractional power-law circuit using OTAs. In *1998 IEEE Asia-Pacific Conference on Circuits and Systems*, TT11-4.1 -4.4, p. 249-252.

[22] MACHADO, J. A. T. Discrete_time fractional-order controllers. *FCAA Journal of Fractional Calculus and Applied Analysis*, 2001, vol. 4, no. 1, p. 47-66.

[23] VLACH, J., SINGHAL, K. *Computer Methods for Circuit Analysis and Design*.2nd edition. Van Nostrand Reinhold, 1994.

About Authors ...

Juraj VALSA was born in 1933 in Czechoslovakia. He received his PhD. from the Military Academy, Brno, Faculty of Communication, in 1965. He devoted most of professional endeavor to computer aided analysis and design of linear and nonlinear electrical, electronic and electromechanical systems. Currently, his research activities cover fractional circuits and systems.

Petr DVOŘÁK was born in Litomyšl, Czech Republic in 1983. He received his Master's degree in Electrical Engineering from the Brno University of Technology in 2007. At present, he is a PhD student at the Department of Electrical and Electronic Technology, Brno University of Technology. His research interests are chemical energy sources.

Martin FRIEDL was born in 1983 in Czech Republic. He received his MSc degree in Electronics, Telecommunication and Control Technique from the Brno University of Technology in 2007. At present, he is a PhD student at the Department of Theoretical and Experimental Electrical Engineering, Brno University of Technology. His main activities are directed to applications of microcontrollers in measurement and signal processing.